

Effects of preparation parameters on oxygen stoichiometry in $\text{Bi}_4\text{V}_2\text{O}_{11-\delta}$ [†]

Isaac Abrahams,^{*a} Alexandra J. Bush,^a Franciszek Krok,^b Geoffrey E. Hawkes,^a Keith D. Sales,^a Peter Thornton^a and Wladyslaw Bogusz^b

^aDept. of Chemistry, Queen Mary and Westfield College, University of London, Mile End Road, London, UK E1 4NS

^bInstitute of Physics, Warsaw University of Technology, ul. Koszykowa 75, 00-662, Warsaw, Poland

The effects of various preparation parameters on vanadium reduction in $\text{Bi}_4\text{V}_2\text{O}_{11-\delta}$ have been investigated using EPR, ⁵¹V MAS solid state NMR and UV diffuse-reflectance spectroscopies and also SQUID magnetometry and powder neutron diffraction. The results confirm that a greater amount of vanadium reduction is observed in rapidly quenched samples and that significant oxidation occurs when samples are slow cooled. Evidence for spin-spin dipolar coupling is seen in the EPR patterns while uncoupled V⁴⁺ spins contribute to weak paramagnetic behaviour. Band gaps of around 2 eV from the UV data suggest there may be a significant electronic component to low temperature conductivities. The ⁵¹V NMR data are not inconsistent with the presence of mainly distorted octahedral and tetrahedral coordinations for vanadium.

Introduction

Fast oxide ion conducting bismuth oxide based compounds have recently become of interest as solid electrolytes for applications in a variety of solid state ionic devices.^{1,2} The materials typically used in such devices are stabilised zirconias which possess good chemical stability but have relatively high operating temperatures, around 1073–1273 K. Certain bismuth oxide based compounds show high conductivities with low activation energies and in some cases have shown conductivities comparable to stabilised zirconias but at significantly lower temperatures.

Bismuth vanadate, $\text{Bi}_4\text{V}_2\text{O}_{11}$, is the parent compound of an extensive range of substitutional solid solutions which have become known as the BIMEVOX family.³⁻⁶ $\text{Bi}_4\text{V}_2\text{O}_{11}$ shows complex polymorphism but essentially has three main polymorphs $\alpha \rightarrow \beta$ (720 K) and $\beta \rightarrow \gamma$ (840 K).⁷ Substitution of V by a host of iso- and alio-valent cations leads to stabilisation of the highly conducting γ -polymorph to room temperature. Conductivities in the order of 10^{-1} S cm⁻¹ have been reported at 873 K for the parent compound⁷ and a number of the substituted BIMEVOXes such as BICOVOX⁸ and BICUVOX.⁹

The idealised structure of $\text{Bi}_4\text{V}_2\text{O}_{11}$ (Fig. 1) consists of alternating layers of $[\text{Bi}_2\text{O}_2]_n^{2n+}$ and $[\text{VO}_{3.5}\blacksquare_{0.5}]_n^{2n-}$, where \blacksquare represents oxide ion vacancies. The $[\text{Bi}_2\text{O}_2]_n^{2n+}$ layers have basal edge-shared BiO_4 square pyramidal groups with the oxygen atoms forming the basal plane and bismuth in the apical position. The vanadate layer in the idealised structure is made up of VO_6 octahedra which corner share in the equatorial plane. This layer is distorted in the real structure of α - $\text{Bi}_4\text{V}_2\text{O}_{11}$.¹⁰ In our recent defect structure determination of the Co doped material BICOVOX,¹¹ it was found that the vacancies in the vanadate layer are concentrated in the equatorial positions around V. In addition distortion of the apical positions yields a structure in which the majority of sites are in fact distorted tetrahedral. In the structure determination of α - $\text{Bi}_4\text{V}_2\text{O}_{11}$ both tetrahedral and octahedral V coordinations were found.¹⁰

The relationship of the three major polymorphs in $\text{Bi}_4\text{V}_2\text{O}_{11}$ can be explained with reference to a mean orthorhombic cell $a_m \approx 5.53$, $b_m \approx 5.61$ and $c_m \approx 15.28$ Å,⁹ for the γ -phase $a = b \approx a_m/\sqrt{2}$, $c \approx c_m$; for the β -phase $a \approx 2a_m$, $b \approx b_m$, $c \approx c_m$; for the α -phase $a \approx 3a_m$, $b \approx b_m$, $c \approx c_m$. The true crystal system of the α -phase however has been the subject of some discussion. It has been found that low levels of cationic impurities present in commercial samples of V_2O_5 result in an orthorhombic phase for α - $\text{Bi}_4\text{V}_2\text{O}_{11}$. However, use of high purity V_2O_5 yields a phase with a small monoclinic distortion which has been crystallographically characterised with a cell $a \approx b_m$, $b \approx c_m$, $c \approx 6a_m$, $\beta = 89.756^\circ$.¹⁰

$\text{Bi}_4\text{V}_2\text{O}_{11}$ is very sensitive to preparation conditions. Preparations by slow cooling and air quenching yield products which are visually different in colour. These colour changes are likely to be due to differences in the electronic structure caused by differing amounts of V⁴⁺. The effect of reduction of V is to increase the total number of oxide vacancies and hence increase the tetrahedral coordination of V. The incorporation of additional vacancies by vanadium reduction may have important effects on the ionic conductivity. The true formula is therefore better written as $\text{Bi}_4\text{V}_2\text{O}_{11-\delta}$.

The value of δ has previously been investigated.¹² Heating samples at 1073 K in air results in a compound with $\delta = 2.5 \times 10^{-2}$, while this increases to 5×10^{-2} under argon. It has

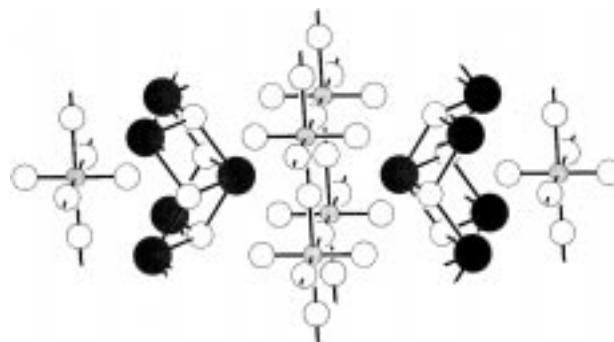


Fig. 1 Idealised layered structure of $\text{Bi}_4\text{V}_2\text{O}_{11}$. Small shaded circles are V, large shaded circles are Bi and unshaded circles are O atoms. Equatorial vacancies are not shown.

[†] Presented at the RSC Autumn Meeting, 2–5 September 1997, University of Aberdeen, Scotland.

been found that samples prepared under a reducing atmosphere of Ar and 10% H₂ yield a compound with one-third of the V reduced, *i.e.* Bi₄V₂O_{10.66} which has a crystal structure best described as Bi₆V₃O₁₆.¹³ Under suitable conditions complete conversion to V^{IV} is possible as in the structure of Bi₄V₂O₁₀.¹⁴ However in this structure all the V are found in square pyramidal coordination.

In this paper various preparation parameters for Bi₄V₂O_{11- δ} , such as slow cooling or air quenching, have been investigated with respect to their effects on V reduction. We have used SQUID magnetometry, neutron diffraction, UV diffuse reflectance spectroscopy, EPR and ⁵¹V solid state NMR to investigate the structural consequences of V reduction in Bi₄V₂O_{11- δ} .

Experimental

Preparation

Bi₄V₂O_{11- δ} was prepared from Bi₂O₃ (Avocado 99%) and V₂O₅ (Aldrich 99.6%) by conventional solid state techniques. Synthesis was carried out by heating a well ground mixture of appropriate molar quantities of the starting materials at 923 K for 6 h in a gold boat and then overnight at 1123 K. In the synthesis of samples, four types of preparation and cooling conditions were adopted as follows: (i) preparation in air and rapid quenching from 1123 K; (ii) preparation in flowing oxygen and exponential slow cooling to room temperature; (iii) preparation in air and exponential slow cooling to room temperature; (iv) preparation in air and linear slow cooling at a rate of 25 °C h⁻¹.

Phase purity was confirmed by X-ray powder diffraction.

Crystallography

High resolution neutron diffraction data on samples i and ii were collected on the HRPD diffractometer at the ISIS facility, Rutherford-Appleton Laboratory. Data were collected at room temperature in back-scattering mode in the TOF range 20–120 ms. The samples were placed in a V-can in the 1 m position. Structure refinement was carried out using the Rietveld method. All calculations were performed using GSAS.¹⁵ A starting model for refinement was based on the idealised orthorhombic mean cell in space group *Aba2*.¹⁶ This approach ignores the weak superlattice reflections but allows for a satisfactory refinement of unit cell contents.

Spectroscopy

⁵¹V magic angle spinning (MAS) solid state NMR data were collected at 157.8 MHz on a Bruker AMX-600 spectrometer using a 4 mm outer diameter rotor, and a spin rate of 12 kHz. The pulse width was 0.7 μ s and 4k points were acquired for each transient, with an acquisition time of 0.02 s and a relaxation delay of 0.5 s. Typically 5000 transients were accumulated for each spectrum. Chemical shifts are reported with the high frequency positive convention and are referenced to external VOCl₃ (= 0 ppm).

UV diffuse-reflectance spectra were collected on a Perkin-Elmer 330 spectrophotometer equipped with a dual channel diffuse reflectance attachment. Relative reflectances of low loaded samples were measured against a white reference.

EPR data were collected on a Bruker 200D X-band spectrometer employing 100 kHz modulation, magnetic field markers from an NMR Gaussmeter and an external microwave frequency counter. All measurements were carried out at room temperature.

Magnetic measurements

SQUID measurements were performed on a Quantum Design MPMS-7 with a magnetic field of 2000 G. Measurements were carried out on samples i, ii and iv.

Results and Discussion

Visible colour changes are observed between slow cooled and rapidly quenched samples. Samples which are furnace cooled in air or oxygen show a deep red colour compared to the quenched samples which are brown. The UV diffuse-reflectance spectra for samples prepared using conditions i–iv is shown in Fig. 2. All samples show strong absorption in the blue region but weaker absorption in the red region. That for the air quenched sample (i) has a stronger absorption in the red region, thus accounting for its darker brown colour. The results show that for slow cooled samples (ii–iv) there is a clear absorption edge around 600 nm whereas in the air quenched samples this absorption edge is less well defined. Clearly the results suggest a difference in electronic structure between slow cooled and rapidly quenched samples. We believe that this difference is caused by small changes in the oxygen stoichiometry and hence the oxidation state of V. In the slow cooled samples clear band edges are visible. For these samples band gap energies were calculated as 1.99, 2.04, and 1.98 eV for samples ii, iii and iv respectively. The air quenched sample (i) did not show a clear band edge and we were therefore unable to calculate a band gap energy for this sample. The band gaps of around 2 eV compare with semiconductors such as CdSe and CdS (1.74 and 2.42 eV respectively at 300 K¹⁷). This suggests that these materials probably show significant electronic semiconducting behaviour at lower temperatures and that the low temperature conductivities may have a significant electronic component. It should be noted however that measurement of oxygen transport numbers between 720 and 1120 K yield a near unity value suggesting that oxide ion conduction predominates at high temperatures.⁷

The nominal +5 oxidation state of V is rarely achieved universally in vanadium oxides, with significant amounts of V⁴⁺ in most commercial samples of V₂O₅. Therefore one expects that in Bi₄V₂O₁₁ a proportion of the vanadium will be in the lower oxidation state V⁴⁺ with an electronic configuration 3d¹. The EPR spectra (Fig. 3) confirm the presence of unpaired electrons in the system.

In the structure determination of BICOVOX we described the likely coordination for V, *viz.* distorted tetrahedra and distorted octahedra.¹¹ The tetrahedral sites arise from equatorial vacancies in the idealised vanadate layer. The axial oxygens are distorted away from their ideal positions, however the total number of oxygens in the axial position is not less than 2 per V. Therefore all oxide ion vacancies are concentrated in the equatorial layer. If only tetrahedral and octahedral coordinations occur, and in Bi₄V₂O₁₁ the defect structure again only shows equatorial vacancies, then the total number of

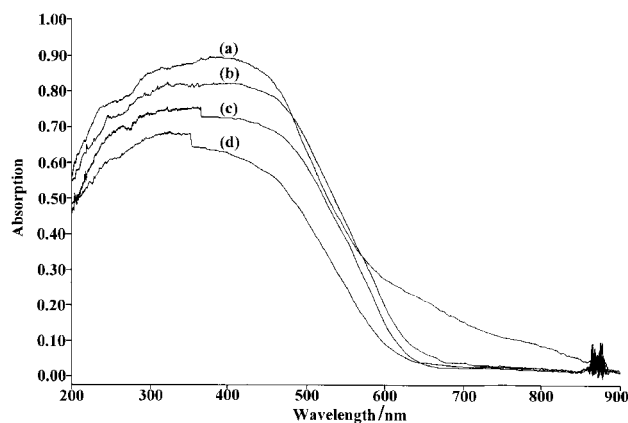


Fig. 2 UV diffuse-reflectance spectra for Bi₄V₂O_{11- δ} prepared by (a) quenching in air (sample i), (b) exponential slow cooling under a dynamic oxygen flow (sample ii), (c) linear slow cooling in air (sample iv) and (d) exponentially slow cooled in air (sample iii)

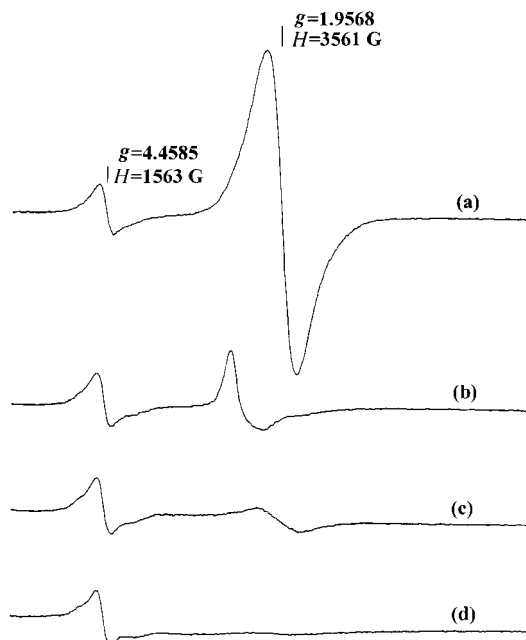


Fig. 3 EPR spectra of $\text{Bi}_4\text{V}_2\text{O}_{11-\delta}$ (a) sample i, (b) sample ii, (c) sample iii, (d) sample iv

tetrahedral sites can be calculated as 0.5 per V. This means that the tetrahedral:octahedral ratio in the idealised V^{5+} system is 1:1. Reduction of the V is likely to introduce further equatorial vacancies and therefore increases the tetrahedral:octahedral ratio.

The powder neutron refinements are summarised in Table 1. As expected sample ii shows a higher oxygen content than sample i, indicating a greater degree of oxidation in the oxygen slow cooled sample. The difference in unit cell volume between the two samples is minimal. This can be explained by considering that any increase in cell volume through incorporation of additional oxygen is balanced by a reduction in size of the vanadium ionic radius in changing from V^{4+} with an ionic radius of 0.46 Å to V^{5+} with an ionic radius of 0.355 Å.¹⁸

From the EPR patterns shown in Fig. 3 it can be seen that the air quenched sample, i, which shows the greatest amount of V reduction, has the strongest signal at a g value of 1.957. Slow cooling in oxygen (sample ii) appears to shift the position of this signal to a g value of 2.235 which is accompanied by a change in line shape. In the case of the two samples slow cooled exponentially in the furnace (samples ii and iii) the signal at higher magnetic field, $g \approx 2$, becomes much weaker

than in the air quenched sample. In the EPR patterns for samples that were slow cooled linearly (sample iv) the higher magnetic field signal was not observed. A half field line was seen in all samples which is likely to result from spin-spin coupling of V^{4+} . This signal at low field was found to have a g value of 4.459 in the air quenched sample and this g value did not vary significantly between samples i-iv. The relative intensities of the resonances vary between samples and reflect the spin concentration. Table 2 summarises the g values for samples i-iv and are in good agreement with a previous study where g values of 1.9543 and 4.3449 were observed.¹⁹

The general features of solid state ^{51}V MAS NMR spectra of oxovanadium(v) compounds have been described by Crans *et al.*²⁰ ^{51}V is a quadrupolar nucleus (spin $I=7/2$) and the MAS spectra are a superposition of the sharper central transition ($m_I = +1/2 \rightarrow m_I = -1/2$) and the six broad satellite transitions. The central transition appears as a central line flanked by spinning side bands, and the intensity pattern for the powdered samples is dominated by the ^{51}V chemical shift anisotropy.^{21,22} Second order quadrupolar effects cause some distortions to the central transition, giving a shift of the central line away from the isotropic chemical shift as well as distortions of the band shape. However, it is expected that the second order quadrupole effects are minimised in spectra measured at the highest magnetic field strengths as obtained here (14.1 T).

The ^{51}V MAS NMR spectra for samples i-iv are shown in Fig. 4. There are two principal centre band resonances (labelled A and B; position invariant with MAS rate) with one weaker high frequency spinning side band (labelled *) from resonance A (there is the possibility of a second high frequency side band). A weak low frequency spinning side band from resonance A is overlapping with resonance B. Other features in the spectra are the weak broad signals of the spinning side band manifold due to the partially excited satellite transitions.²¹ The lack of a widespread manifold of spinning side bands for either A or B indicates that these resonances have modest values for the chemical shift anisotropy (200–300 ppm). Resonance B is

Table 2 g values calculated from the EPR spectra of samples i-iv

sample	half field line	$g \approx 2$ line
air quenched (sample i)	4.459	1.957
oxygen slow cooled exponentially (sample ii)	4.485	2.235
slow cooled in air exponentially (sample iii)	4.465	1.960
slow cooled in air linearly (sample iv)	4.487	—

Table 1 Refined atomic parameters from the room temperature neutron diffraction profiles of (a) $\text{Bi}_4\text{V}_2\text{O}_{11-\delta}$ quenched in air [sample (i)] and (b) $\text{Bi}_4\text{V}_2\text{O}_{11-\delta}$ exponentially slow cooled in oxygen [sample (ii)] (estimated standard deviations are given in parentheses)

atom	x/a	y/b	z/c	occupancy	$U_{\text{iso}}/\text{Å}^2$
(a) sample (i) ^a					
Bi(1)	0.4968(8)	0.1688(2)	0.000(—)	1.00(—)	0.0346(9)
V(1)	0.000(—)	0.000(—)	0.0508(—)	1.00(—)	0.025(—)
O(1)	0.243(3)	0.2502(5)	0.263(2)	1.00(—)	0.0215(9)
O(2)	0.335(3)	0.506(3)	0.308(3)	0.55(2)	0.085(3)
O(3)	−0.064(1)	0.1005(6)	0.046(3)	1.00(—)	0.085(2)
(b) sample (ii) ^b					
Bi(1)	0.493(1)	0.1690(2)	0.000(—)	1.00(—)	0.0156(9)
V(1)	0.000(—)	0.000(—)	0.0508(—)	1.00(—)	0.025(—)
O(1)	0.243(3)	0.2458(8)	0.263(3)	1.00(—)	0.007(1)
O(2)	0.316(2)	0.511(2)	0.303(3)	0.63(2)	0.056(3)
O(3)	−0.067(1)	0.0997(6)	0.051(3)	1.00(—)	0.056(3)

^a $R_{\text{WP}}=17.13\%$, $R_{\text{P}}=14.37\%$, $R_{\text{EX}}=2.13\%$, for 6020 data points and 570 reflections. $a=5.5827(2)$, $b=15.2283(6)$, $c=5.5073(2)$ Å, $V=468.20(5)$ Å³. ^b $R_{\text{WP}}=10.36\%$, $R_{\text{P}}=8.26\%$, $R_{\text{EX}}=1.92\%$, for 6020 data points and 572 reflections. $a=5.5840(3)$, $b=15.2218(9)$, $c=5.5080(3)$ Å, $V=468.16(7)$ Å³. For definition of R -factors see ref. 26.

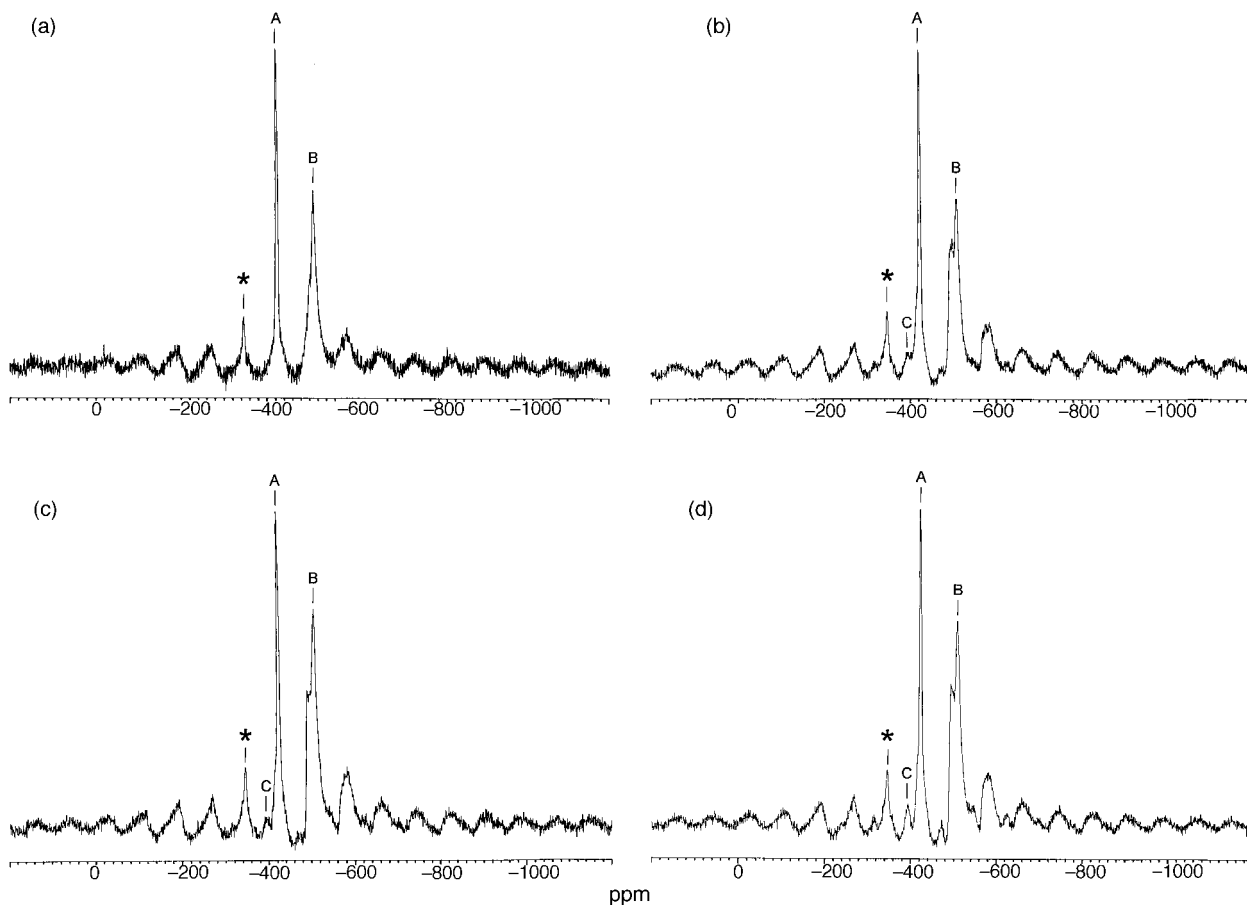


Fig. 4 Solid state ^{51}V NMR spectra for $\text{Bi}_4\text{V}_2\text{O}_{11-\delta}$, (a) sample i, (b) sample ii, (c) sample iii, (d) sample iv. Resonances for distorted tetrahedral (A), octahedral (B) and square pyramidal (C) vanadium sites are indicated.

clearly broader than A and there is evidence of splitting of B [Fig. 4(b)–(d)] in some of the spectra. The possibility exists that this apparent splitting is the result of second order quadrupole effects on the band shape for a single resonance or, more likely, it is the result of two quite similar environments.

Previously collated ^{51}V NMR data have shown that, typically, resonances from tetrahedral vanadium display lower values for the chemical shift anisotropy than octahedrally coordinated vanadium,²³ however these values depend critically upon the symmetry around vanadium. Therefore, the isotropic ^{51}V chemical shift alone is not an absolute indicator of vanadium coordination number. Crystallographic data¹⁰ indicate the presence of both four and six coordinate vanadium and the observed uncorrected shift for resonance A is -423 ppm, which is similar to the isotropic shift reported for BiVO_4 (tetrahedral vanadium).²² The observed uncorrected shift for resonance B occurs at -510 ppm and compares with literature values for distorted octahedral oxovanadium of -500 to -536 ppm.²² We therefore assign resonance A to tetrahedral vanadium and B to octahedral vanadium. The chemical shift anisotropy for resonance A is within the range derived by Crans *et al.*²⁰ for distorted four or five coordinate vanadium sites, while distorted six coordinate sites were reported by these authors to have somewhat higher values for the chemical shift anisotropy in the range 500 – 700 ppm. The relative magnitudes of the chemical shift anisotropies for sites A and B indicate that both these sites are somewhat distorted away from regular coordination geometry, which is consistent with the crystallographic evidence.

In slow cooled samples a third resonance, C, is observed centred at around -398 ppm. We believe that this third resonance may be due to low levels of five coordinate

vanadium. It is known that in the structure of $\text{Bi}_4\text{V}_2\text{O}_{10}$, *i.e.* the fully reduced system, all the vanadium is five coordinate in square pyramidal coordination,¹⁴ and it is highly likely that in the partially reduced system some five coordinate vanadium will be present.

These assignments are in contrast to those of Hardcastle *et al.*²⁴ who in a study of the composition range $1:1-60:1$ $\text{Bi}_2\text{O}_3\text{-V}_2\text{O}_5$ assigned a peak at approx. -425 ppm to BiVO_4 and a peak at -510 ppm to the tetrahedral site in $\text{Bi}_4\text{V}_2\text{O}_{11}$. Our diffraction evidence suggests that there are not significant amounts of BiVO_4 present in the sample and therefore both peaks are due to the main phase $\text{Bi}_4\text{V}_2\text{O}_{11}$. Their original assignment was based on the assumption that the structure of $\text{Bi}_4\text{V}_2\text{O}_{11}$ contained V in entirely tetrahedral coordination. It has since been shown that in the low temperature monoclinic form of $\alpha\text{-Bi}_4\text{V}_2\text{O}_{11}$ both tetrahedral and octahedral V sites are present.¹⁰

Susceptibility plots for samples i, ii and iv, derived from the SQUID data, are shown in Fig. 5. Samples i and ii show classic paramagnetic behaviour with low overall magnetic susceptibilities. This paramagnetism is attributable to a small number of uncoupled V^{4+} spins. A small kink in the curves is seen in the 50 – 70 K region due to residual oxygen in the sample holder. This effect is normally swamped in concentrated spin systems but is observed here due to the relatively small magnetisation. The relatively low magnitude of susceptibility observed in sample iv suggests that in this material there is a low uncoupled spin concentration. The half field lines in the EPR data which are indicative of spin–spin coupling were observed in all samples including sample iv, where the main high field signal was absent. Therefore it can be concluded that although the SQUID data reveal information on the nature of the uncoupled

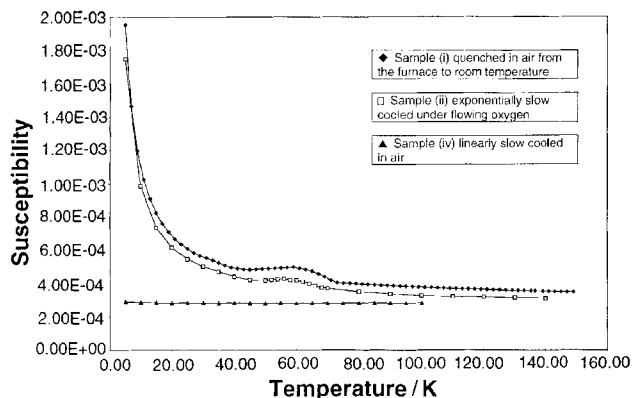


Fig. 5 Susceptibility plots of $\text{Bi}_4\text{V}_2\text{O}_{11-\delta}$, synthesised by various preparation parameters, derived from the SQUID data

V^{4+} spins in this weak system they cannot be easily related to the overall V^{4+} concentration because of the extent of spin-spin coupling.

An important consequence of significant V reduction is that it imposes a lower solid solution limit in the substituted BIMEVOXes when compared to the ideal situation of a fully oxidised system. Considering BIMEVOX solid solutions of general formula $\text{Bi}_2\text{V}_{1-x}\text{M}_x\text{O}_{5.5-3x/2}$ (where M is a divalent metal); in the ideal case where V is fully oxidised to V^{5+} and assuming that the solid solution mechanism involves creation of only equatorial vacancies, as observed in the BICOVOX structure,¹¹ the limit for solid solution formation will be when all the possible vacancies are introduced, *i.e.* when all the V sites are tetrahedral. This can be calculated to occur at $x=0.33$. Generally for divalent substitution a lower solid solution limit of around $x=0.25$ is usually observed.³ However, Lee *et al.*²⁵ have shown that for $\text{M}=\text{Co}$ this can be extended to the maximum of $x=0.33$. Observed lower solid solution limits in other systems suggest that further vacancy creation does not occur and that a possible explanation is that many of these additional vacancies have already been created through V reduction. However, it is unlikely that these lower solid solution limits can be explained entirely by this mechanism as this would imply unreasonably high V^{4+} concentrations. It may well be the case that thermodynamic considerations are the predominant factor in determining the solid solution limit.

Conclusions

We have shown that oxygen stoichiometry in $\text{Bi}_4\text{V}_2\text{O}_{11-\delta}$ is greatly affected by preparation parameters. Air quenching of samples preserves a high V^{4+} concentration, with slow cooling methods in air or oxygen increasing the amount of oxidation. While we have not been able to directly measure the value of δ in this study, our results suggest that there is a significant amount of V reduction and is reflected in the observed differences in colour, magnetisation, EPR signal strength and unit cell contents. ^{51}V NMR spectroscopy is not inconsistent with the presence of mainly distorted tetrahedral and distorted octahedral coordination geometry for vanadium in all samples irrespective of preparation conditions with small amounts of

square pyramidal vanadium appearing in slow cooled samples. The relatively small band gaps of around 2 eV suggest that low temperature conductivities may have a significant electronic component.

We gratefully acknowledge the EPSRC for a project studentship to A.J.B. and for use of the ISIS facility at the Rutherford-Appleton Laboratory. We would like to thank Professor P. Day and Dr. S. G. L. Carling at The Royal Institution of Great Britain for use of the SQUID magnetometer, Dr. A. Aliev using the ULIRS Solid State NMR 600 MHz service at QMW and Dr. D. Oduwole at the ULIRS EPR service at QMW.

References

- 1 N. Q. Minh, *J. Am. Ceram. Soc.*, 1993, **76**, 563.
- 2 J. B. Goodenough, A. Manthiram, M. Paranthaman and Y. S. Zhen, *Mater. Sci. Eng. B*, 1992, **12**, 357.
- 3 F. Abraham, J. C. Boivin, G. Mairesse and G. Nowogrocki, *Solid State Ionics*, 1990, **40/41**, 934.
- 4 G. Mairesse, in *Fast Ion Transport in Solids*, ed. B. Scrosati, A. Magistris, C. M. Mari and G. Mariotto, Kluwer, Dordrecht, 1993, p.271.
- 5 J. C. Boivin, R. N. Vannier, G. Mairesse, F. Abraham and G. Nowogrocki, *ISSI Lett.*, 1992, **3**, 14.
- 6 S. Lazure, Ch. Vernochet, R. N. Vannier, G. Nowogrocki and G. Mairesse, *Solid State Ionics*, 1996, **90**, 117.
- 7 F. Abraham, M. F. Debreuille-Gresse, G. Mairesse and G. Nowogrocki, *Solid State Ionics*, 1988, **28-30**, 529.
- 8 F. Krok, W. Bogusz, W. Jakubowski, J. R. Dygas and D. Bangobango, *Solid State Ionics*, 1994, **70/71**, 211.
- 9 E. Pernot, M. Anne, M. Bacmann, P. Strobel, J. Fouletier, R. N. Vannier, G. Mairesse, F. Abraham and G. Nowogrocki, *Solid State Ionics*, 1994, **70/71**, 259.
- 10 O. Joubert, A. Jouanneaux and M. Ganne, *Mater. Res. Bull.*, 1994, **29**, 175.
- 11 I. Abrahams, F. Krok and J. A. G. Nelstrop, *Solid State Ionics*, 1996, **90**, 57.
- 12 M. Huve, R. N. Vannier, G. Nowogrocki, G. Mairesse and G. Van Tendeloo, *J. Mater. Chem.*, 1996, **6**, 1339.
- 13 O. Joubert, A. Jouanneaux and M. Ganne, *Nucl. Instrum. Methods Phys. Res. B*, 1995, **97**, 119.
- 14 J. Galy, R. Enjalbert, P. Millan and A. Castro, *C. R. Acad. Sci. Paris, Ser. II*, 1993, **317**, 43.
- 15 A. C. Larson and R. B. Von Dreele, Los Alamos National Laboratory Report No. LAUR-86-748, 1987.
- 16 *International Tables for Crystallography, Volume A*, ed. T. Hahn, IUCR, Kluwer, Dordrecht, 1992.
- 17 C. Kittel, in *Introduction to Solid State Physics*, John Wiley and Sons, Chichester, 1976, 5th edn., p.210.
- 18 R. D. Shannon and C. T. Prewitt, *Acta Crystallogr., Sect. B*, 1969, **25**, 925.
- 19 A. Aboukais, F. Delmaire, M. Rigole, R. Hubaut and G. Mairesse, *Chem. Mater.*, 1993, **5**, 1819.
- 20 D. C. Crans, R. A. Felty, H. Chen, H. Eckert and N. Das, *Inorg. Chem.*, 1994, **33**, 2427.
- 21 R. H. H. Smits, K. Seshan, J. R. H. Ross and A. P. M. Kentgens, *J. Phys. Chem.*, 1995, **99**, 9169.
- 22 H. Eckert and I. E. Wachs, *J. Phys. Chem.*, 1989, **93**, 6796.
- 23 O. R. Lapina, V. M. Mastikhin, A. A. Shubin, V. N. Krasilnikov and K. I. Zamaraev, *Prog. NMR. Spectrosc.*, 1992, **24**, 457.
- 24 F. D. Hardcastle, I. E. Wachs, H. Eckert and D. A. Jefferson, *J. Solid State Chem.*, 1991, **90**, 194.
- 25 C. K. Lee, G. S. Lim and A. R. West, *J. Mater. Chem.*, 1994, **4**, 1441.
- 26 H. M. Rietveld, *J. Appl. Crystallogr.*, 1969, **2**, 65.

Paper 8/01614C; Received 25th February, 1998